STIM1-regulated exosomal EBV-LMP1 empowers endothelial cells with aggressive phenotype by activating the Akt/ERK pathway in nasopharyngeal carcinoma

Yayan Deng
Guangxi Medical University Cancer Hospital
Xue Liu
Guangxi Medical University Cancer Hospital
Yujuan Huang
Guangxi Medical University Cancer Hospital
Jiaxiang Ye
Guangxi Medical University Cancer Hospital
Qian He
Tsinghua Shenzhen International Graduate School
Yue Luo
Guangxi Medical University Cancer Hospital
Yong Chen
Guangxi Medical University Cancer Hospital
Qiuyun Li
Guangxi Medical University Cancer Hospital
Yan Lin
Guangxi Medical University Cancer Hospital
Rong Liang
Guangxi Medical University Cancer Hospital
Yongqiang Li
Guangxi Medical University Cancer Hospital
Jiazhang Wei
The People's Hospital of Guangxi Zhuang Autonomous Region
Jinyan Zhang (zhangjinyan@gxmu.edu.cn)
Guangxi Medical University Cancer Hospital

Research Article

Keywords: Stromal interaction molecule 1, Angiogenesis, Latent membrane protein 1, Nasopharyngeal carcinoma, Tumor-derived exosomes

Posted Date: March 7th, 2023

DOI: https://doi.org/10.21203/rs.3.rs-2341571/v1

Abstract

Background Stromal interaction molecule 1 (STIM1)-mediated Ca^{2+} signaling regulates tumor angiogenesis in nasopharyngeal carcinoma (NPC), an Epstein-Barr virus (EBV)-related human malignancy. However, the mechanism by which STIM1 modulates the endothelial functional phenotypes contributing to tumor angiogenesis remains elusive.

Methods We explored the intercellular communication via exosomal biomolecules released by EBV-infected NPC cells and delivered to endothelial cells (ECs). The NPC cell-derived exosomes were isolated via differential centrifugation and observed with transmission electron microscopy. Exosome particle size was assessed by nanoparticle tracking analysis (NTA). Uptake of exosomes by recipient ECs was detected by fluorescent labeling of the exosomes with PKH26. Tumor angiogenesis-associated profiles were characterized by determining cell proliferation, migration, tubulogenesis, and permeability in human umbilical vein endothelial cells (HUVECs). Activation of the Akt/ERK pathway was elucidated by detecting the phosphorylation level using western blotting. A chick embryo chorioallantoic membrane (CAM) xenograft model was employed to study tumor-associated neovascularization *in vivo*.

Results The NPC cell-derived exosomes harboring EBV-encoded latent membrane protein 1 (LMP1) promoted proliferation, migration, tubulogenesis, and permeability by activating the Akt/ERK pathway in ECs. STIM1 silencing reduced LMP1 enrichment in NPC cell-derived exosomes, thereby reversing its pro-oncogenic effects in an Akt/ERK pathway-dependent manner. Furthermore, STIM1 knockdown in NPC cells blunted tumor-induced vascular network formation and inhibited intra-tumor neovascularization in the chorioallantoic membrane (CAM) xenograft model.

Conclusion STIM1 regulates tumor angiogenesis by controlling exosomal EBV-LMP1 delivery to ECs in the NPC tumor microenvironment. Blocking exosome-mediated cell-to-cell horizontal transfer of EBV-associated oncogenic signaling molecules may be an effective therapeutic strategy for NPC.

1 Introduction

Nasopharyngeal carcinoma (NPC) is an Epstein-Barr virus (EBV)-related head and neck squamous cell carcinoma (HNSCC) with unusual geographical and ethnic distributions worldwide[1, 2]. NPC is the most common HNSCC in southern China, with a particularly high incidence in the Cantonese-speaking population[3, 4]. Multiple factors synergistically contribute to NPC pathogenesis, including genomic instability, genetic susceptibility, and latent EBV infection[1, 2]. The latter participates in NPC development by shaping malignant phenotypes and reprogramming cellular metabolism in the infected host epithelial cells. EBV infection also contributes to NPC progression by remodeling the tumor microenvironment (TME), which causes deregulated proliferation, regional invasiveness, and ultimately distant dissemination of NPC cells[5–9].

Exosomes, a class of extracellular vesicles harboring a variety of bioactive molecules, serve as pivotal mediators of cell-cell communication in the TME[10, 11]. The EBV-encoded latent membrane protein 1

(LMP1) can be sorted and loaded into exosomes released by EBV-infected cells, which are then uptaken by the surrounding non-EBV-infected cells, including endothelial cells (ECs) [12–15]. However, the effects of exosomal LMP1 on EC functional phenotypes that contribute to tumor angiogenesis remain poorly understood.

Previously, we reported that stromal interaction molecule 1 (STIM1)-dependent store-operated Ca^{2+} entry (SOCE) mediates LMP1-promoted cell-cell interaction between NPC cells and neighboring ECs [16]. Our next study showed that EBV infection enhances tumor angiogenesis by boosting STIM1-mediated Ca^{2+} signaling[17, 18]. Amplified Ca^{2+} influx increasing cytosolic Ca^{2+} concentration triggers the docking and fusion of multivesicular bodies and stimulates exosome release [19–21]. Elevated STIM1-mediated Ca^{2+} entry enhances exosome release to the extracellular matrix [22]. Even so, the regulatory role of STIM1 in exosome-mediated intercellular communication between NPC cells and ECs, as well as the effects of exosomal delivery of oncogenic signals on endothelial features, remain elusive.

In the present study, we demonstrated that NPC cell-derived exosomes carrying LMP1 promoted proliferation, migration, tubulogenesis, and permeability by stimulating the Akt/ERK pathway in ECs. Silencing STIM1 in EBV-infected NPC cells decreased LMP1 loading into exosomes, which further blunted the effects of exosomal LMP1 on EC characteristics responsible for tumor angiogenesis. Using a modified chick embryo chorioallantoic membrane (CAM) model, we showed that silencing STIM1 inhibited xenograft-induced vascular network formation and intra-tumor neovascularization.

2 Materials And Methods

2.1 Cell culture

The EBV-positive NPC cell lines HK1-EBV (RRID: CVCL_7084) and C666-1 (RRID: CVCL_7949) were gifted by Prof. Sai-Wah Tsao (Hong Kong University, Hong Kong, China) and Prof. Musheng Zeng (Sun Yat-sen University Cancer Center, Guangzhou, China). HK1-EBV cells were cultured in Dulbecco's Modified Eagle Medium supplemented with 10% fetal bovine serum (FBS), 100 U/mL penicillin, and 100 μg/mL streptomycin (Invitrogen, Thermo Fisher Scientific Corp., Carlsbad, CA, USA). C666-1 cells were cultured in Roswell Park Memorial Institute 1640 medium supplemented with 10% FBS and antibiotics as described above. Human umbilical vein endothelial cells (HUVECs; CRL-1730TM; American Type Culture Collection; Manassas, Virginia, USA) were cultured in EC Medium (Scien Cell, San Diego, CA, USA) containing 5% FBS and antibiotics. All cells were routinely maintained in an incubator at 37°C under 5% CO_2. The HK1-EBV and C666-1 cells used in our study were authenticated using short-tandem repeat profiling to confirm the identity of the cell lines as described in previous studies [23, 24].

2.2 Exosome isolation, transmission electron microscopy, and nanoparticle tracking analysis (NTA)

A total of 5×10^6 HK-EBV or C666-1 cells were seeded in a 150 mm dish. When cells reached approximately 70% confluence, they were incubated in serum-free medium for 12 h, which was replaced with serum-free medium containing 50 ng/mL recombinant human epidermal growth factor (PeproTech, Cranbury, NJ, USA) for 36 h, and the cell supernatants were harvested. Exosomes were isolated and collected via differential centrifugation at 300 ×g for 10 min, 2,000 ×g for 15 min, 10,000 × g for 30 min, and ultracentrifugation at 100,000 ×g for 90 min. All centrifugations were performed at 4°C. The exosomes were washed once with phosphate-buffered saline (PBS) and subjected to a second ultracentrifugation under the same conditions. The isolated exosomes were resuspended in PBS and stored at -80°C before subsequent experiments.

The morphological characteristics of the exosomes were observed via transmission electron microscopy (Hitachi HC-1, Japan) at an accelerating voltage of 80 kV. Exosome particle size was assessed via NTA using Particle Metrix ZetaView (Shanghai Biochip Co., Ltd., Shanghai, China) according to the manufacturer's instructions. A bicinchoninic acid protein assay kit (Beyotime Biotechnology, Shanghai, China) was used to quantify exosome protein content. For *in vitro* experiments, 10 μg/mL exosomes were incubated with recipient cells.

2.3 Exosome labeling and uptake by recipient cells

The PKH26 linker stock solution was diluted with Diluent C according to the manufacturer's instructions (Umibio Co., Ltd., Shanghai, China, Cat. No: UR52302) to prepare a working dye solution with a concentration of 100 μmol/L. The purified exosomes were incubated with the working dye solution for 10 min and then ultracentrifuged at 100,000 ×g for 90 min to remove excess dye. After centrifugation, resuspended PKH26-labeled exosomes were incubated with recipient ECs for 24 h and observed via confocal microscopy (Molecular Devices, California, USA).

2.4 Cell proliferation assay

The Cell Counting Kit-8 (CCK-8) assay and 5-ethynyl-2'-deoxyuridine (EdU) fluorescent staining were used to evaluate the proliferative capacity of HUVECs. A total of 2.0×10^3 HUVECs were seeded in each well of 96-well plates. After complete cell adhesion was achieved, the medium supplemented with FBS was replaced with a medium containing 10 μg/mL exosomes or PBS (vehicle control), and the cells were allowed to grow continually. Ten microliters CCK-8 reagent solution (Dalian Meilun Biotechnology Co., Ltd., Dalian, China, Cat. No: MA0218-5) was added to each well at 0, 24, 48, 72, and 96 h and incubated at 37 ℃ for 3 h. The absorbance of each well was measured at 450 nm wavelength using a microplate reader (Tristar LB941, Berthold Technologies, Germany). For EdU fluorescent staining, a total of 2.0×10^4 HUVECs were seeded in 24-well plates containing 10 μg/mL exosomes and 5% FBS. After 72 h of incubation, the medium was discarded, and medium containing 50 μmol/L EdU (Guangzhou RiboBio Co., Ltd., Guangzhou, China, Cat. No. C10310-1) was added to each well. After 4 h of incubation at 37 ℃, the cells were fixed with 4% paraformaldehyde, stained with Apollo and Hoechst, and photographed under a fluorescence microscope (IX2-ILL100, Olympus Corp., Tokyo, Japan). The number of EdU-positive cells was calculated as the percentage of total cells per random field.

2.5 *In vitro* migration assay

HUVEC migration ability was evaluated via wound healing and transwell migration assays, as described in our earlier works[16, 25]. A total of 1.5×10^5 HUVECs were seeded into each well of a 24-well plate containing 5% FBS. When the cells reached 90% confluence, the monolayer was scraped off using a sterile pipette tip to form a gap. Serum-free medium containing 10 μg/mL exosomes or PBS was added for incubation, and photographs of the same viewing field were obtained 48 h later. The percentage of the wound healing area was calculated using ImageJ. To conduct the transwell migration assay, 3.0×10^5 HUVECs were inoculated into 6-well plates containing 10 μg/mL exosomes and 5% FBS for 72 h. Then, 1.0×10^5 HUVECs were resuspended in 200 μL serum-free medium and added to each 8 μm-pore size transwell chamber (Corning, NY, USA), then placed in 24-well plates containing 20% FBS. After 48 h of incubation at 37°C, the upper chambers were carefully removed, and the cells on the lower surface of the membrane were fixed with 4% paraformaldehyde and stained with 0.1% crystal violet. The cells were photographed under a microscope (IX2-ILL100, Olympus Corp.), and ImageJ software was used to count the number of membrane-crossing cells in each random field.

2.6 *In vitro* tube formation assay

Tube formation assays were performed to evaluate the EC tube-forming ability, as described in our previous studies[17, 18]. Briefly, 3.0×10^5 HUVECs were seeded into each well of a 6-well plate containing 10 μg/mL exosomes and 5% FBS and incubated for 72 h. After 50 μL of Matrigel (Corning, NY, USA, Cat. No: 356234) was applied to each well of a 96-well plate and allowed to solidify, 100 μL of the cell suspension at a density of 4.0×10^5/mL pretreated with exosomes was seeded into each well. After 18 h of incubation at 37°C, endothelial tube formation was observed and photographed under a microscope (IX2-ILL100, Olympus Corp.). The number of tube rings in each random field was calculated to evaluate the tube-forming capacity of HUVECs pretreated with exosomes.

2.7 Fluorescein isothiocyanate (FITC)-labeled dextran permeability assay

The permeability of the endothelial layer formed by HUVECs treated with exosomes was determined as reported in our previous study [16]. A total of 5.0×10^4 HUVECs were resuspended in a medium containing 10 μg/mL exosomes, which were added into 0.4 μm-pore size upper chambers (Corning, NY, USA). The chambers were placed in 24-well plates containing 5% FBS. After 96 h of incubation, the ECs fused to form a monolayer, as confirmed via microscopic observation, and the medium was aspirated and discarded. Serum-free and phenol red-free medium containing FITC-dextran (Sigma-Aldrich Trading Co., Ltd., Shanghai, China, Cat. No. 46945) at 1 mg/mL was added to the upper chamber, while serum- and phenol red-free medium was added to each well of the plates. The medium in each bottom well was collected and transferred to a light-proof 96-well plate, and the absorbance of the medium at 488 nm was measured using a microplate reader at 0, 20, 40, and 60 min (Infinite 200 Pro, Tecan Trading AG, Switzerland).

2.8 STM1 knockdown via lentiviral vector transfection

The recombinant plasmid vector GV248 containing STIM1-RNA interference (shRNA-STIM1, GGGAA GACCTCAATTACCA) or a nonsense scrambled sequence (shRNA-Ctrl., TTCTCCGAACGTGTCACGT) was purchased from GeneChem Technology (Shanghai, China). Lentivirus transfection was performed according to the manufacturer's instructions. The reduction in STIM1 expression was validated via western blotting.

2.9 Western blotting

Total cell proteins or exosome total proteins were separated using 10% sodium dodecyl sulfate-polyacrylamide gel electrophoresis and transferred to a polyvinylidene difluoride membrane. The membranes were blocked with rapid blocking solution for 15 min at room temperature and incubated with the primary antibodies at 4°C overnight. Membranes were then incubated with horseradish peroxidase-conjugated secondary antibodies for 1 h at room temperature. The bands in the gel were visualized using enhanced chemiluminescence and photographed. The antibodies used in this study included GAPDH (1:1000; Servicebio, Cat. No. GB11002), STIM1 (1:1000; Abmart; Cat. No: #M25012), LMP1 (1:2000; Abcam, Cat. No: ab78113), CD63 (1:1000; Abcam, Cat. No: ab134045), TSG101 (1:1000; Abcam, Cat. No: ab125011), HSP70 (1:1000; Abcam, Cat. No: ab181606), Akt (1:1000; Abcam, Cat. No: ab184699), phosphorylated Akt (p-AKT; 1:1000; Abmart, Cat. No: TA3262), ERK (1:10,000; Abcam, Cat. No. ab184699), and phosphorylated ERK (p-ERK; 1:400; Abcam, Cat. No. ab223500).

2.10 Chick embryo CAM xenograft model

All animal experiments performed in this study were approved by the Animal Research Committee of Guangxi Medical University and carried out according to the regulations of the Animal Research Committee of Guangxi Medical University. A CAM xenograft model was established to observe the malignant behavior of NPC cells *in vivo* in our previous study [26] and employed to explore the transplanted tumor-induced vascular network formation and intra-tumor neovascularization with slight modifications. Fertilized Fufeng eggs (Guangxi Fufeng Trading Group Co., Ltd., Nanning, China) were routinely incubated at 38°C and 60% humidity. Briefly, a window (2.0 × 2.0 cm) in the eggshell air chamber was made on the eighth day of incubation for inoculation and observation. A total of 2.0×10^6 HK1-EBV cells transfected with shRNA-Ctrl. or shRNA-STIM1 suspended in 30 μL of Matrigel (Corning, NY, USA) were inoculated into the CAM through the window. The eggshell windows were sealed with an applicator of the appropriate size. Transplanted tumor angiogenesis and embryo viability were observed daily via *in situ* photography. After five days of inoculation, the membranes were peeled off with the xenografts in the center, and tumor angiogenesis was evaluated by calculating the ratio of the blood vessel area to the entire CAM area using the Image-Pro Plus 6 analysis system, as previously described [27]. CAM xenografts were fixed with 4% paraformaldehyde and embedded in paraffin, followed by hematoxylin and eosin (H&E) staining and immunohistochemistry (IHC).

2.11 Primary NPC tissues and immunofluorescence

This study was approved by the ethics committee of Guangxi Medical University Cancer Hospital (Ref: KY2020014), and informed consent was obtained from all patients. This study complied with the principles of the Declaration of Helsinki. A total of 11 primary tumor tissues were collected from patients pathologically diagnosed with undifferentiated non-keratinizing nasopharyngeal carcinoma (WHO classification, type III) before treatment for immunofluorescence staining analysis. All tumor tissues were tested for EBV-encoded mRNA (EBER) and showed a positive reaction. After routine dewaxed rehydration, antigen repair, and serum blocking, the sections were incubated with anti-LMP1 (1:200, Santa Cruz Biotechnology, Cat. No: SC-71023), and anti-human CD31 (1:100; Servicebio, Cat. No: GB11063-1) antibodies overnight at 4°C. Goat anti-rabbit IgG (H + L) was conjugated to Alexa Fluor® 488 (1:4000; Servicebio, Cat. No: GB25303) or cy3-labeled goat anti-mouse IgG (H + L) (1:300, Servicebio, Cat. No. GB25303) antibodies and incubated at room temperature. Cell nuclei were counterstained with DAPI, and images were acquired using a fluorescence microscope (NIKON ECLIPSE C1, Nikon, Japan).

2.12 Statistical analysis

SPSS24.0 (IBM, Chicago, IL, USA) and Graphpad prism 8.0 (GraphPad, San Diego, CA, USA) were used for statistical analyses. Data are presented as means ± SD. Student's *t*-test or two-way ANOVA was used for statistical analyses, and statistical significance was assumed at $P < 0.05$.

3 Results

3.1 Exosomes released from EBV-positive NPC cells harbor LMP1

LMP1 can be loaded into exosomes and secreted by EBV-infected host cells into the TME [12]. To investigate the role of exosomal LMP1 in remodeling endothelial functional phenotypes contributing to tumor angiogenesis, we first isolated the exosomes released by two EBV-positive NPC cell lines, HK1-EBV and C666-1, via differential centrifugation from the cell-conditioned medium (Fig. 1a). NTA indicated that exosome diameter was mainly distributed in the range of 100–200 nm (Fig. 1b). Transmission electron microscopy revealed that the isolated exosomes exhibited typical morphological characteristics of lipid bilayer vesicles (Fig. 1c). Western blotting was performed to detect various exosome-specific markers, such as CD63, TSG101, and HPS70, and the presence of LMP1 in NPC cell-derived exosomes was confirmed (Fig. 1d).

3.2 EBV-LMP1 transferred to ECs via NPC cell-derived exosomes correlates with tumor angiogenesis

Tumor cell-derived exosomes were labeled with the lipophilic membrane dye PKH26 (Fig. 2a). After 24 h of incubation, PKH26-labeled exosomes were taken up by HUVECs, as shown in the representative fluorescence microscopic images (Fig. 2a). EBV-LMP1 functions as a proangiogenic oncoprotein and correlates with tumor angiogenesis [5, 16, 28]. To further explore the contribution of LMP1 to tumor angiogenesis in NPC, we performed immunofluorescence staining of the EBV-positive primary tumor tissues. We validated that LMP1 is colocalized with CD31-positive vascular ECs or is highly expressed in perivascular NPC cells. Two representative immunofluorescence images of sections from two independent patients with NPC are shown in Fig. 2b.

3.3 Exosomes harboring LMP1 modulate endothelial functional phenotypes

Next, we studied the effects of NPC cell-derived exosomes carrying LMP1 on the functional characteristics contributing to tumor angiogenesis in ECs *in vitro*. HUVECs were incubated with exosomes extracted from the conditioned medium of NPC cells. LMP1-containing exosomes promoted HUVEC proliferation and migration (Fig. 3a-3d). Moreover, tumor exosomes significantly enhanced the tube-forming ability of HUVECs and permeabilized the endothelial layer (Fig. 3e, 3f). We further evaluated the activation of the Akt/ERK signaling pathway by detecting Akt and ERK phosphorylation levels. Western blotting showed that p-AKT and p-ERK expression levels increased in HUVECs incubated with exosomes for 72 h (Fig. 3g). These results suggest that NPC cell-derived exosomes modulate the endothelial functional phenotypes responsible for tumor angiogenesis through the Akt/ERK pathway.

3.4 STIM1 regulates tumor angiogenesis by controlling EBV-LMP1 delivery

Exosome release is regulated by changes in cytosolic Ca^{2+} level [19–21], and it was recently reported that STIM1-mediated Ca^{2+} signaling manipulates the release of exosomal matrix proteins [22]. However, the regulatory role of STIM1 in exosomal EBV-LMP1 delivery remains to be further clarified. To address this issue, we established stable STIM1-silencing NPC cells lines by transfecting HK1-EBV and C666-1 cells with lentiviral vectors carrying scrambled shRNA (shRNA-Ctrl.) or STIM1-RNAi (shRNA-STIM1) sequences. Reduced STIM1 expression in NPC cells was confirmed via western blotting (Fig. 4a). The exosomal marker content was also detected in the exosomes extracted from the conditioned medium of shRNA-Ctrl. and shRNA-STIM1 cells (Fig. 4a). Moreover, the amount of LMP1 in the exosomes released from shRNA-STIM1 cells was significantly lower than that released from shRNA-Ctrl. cells (Fig. 4a). Thus, we further investigated whether exosomal LMP1 modulates angiogenesis-related features in ECs. The promotion of HUVEC proliferation, migration, tubulogenesis, and permeability after treatment with exosomes was significantly blunted in the shRNA-STIM1 group (Fig. 4b-4g). We also found that Akt and ERK phosphorylation was attenuated in HUVECs incubated with exosomes secreted from shRNA-STIM1 cells (Fig. 4h). Taken together, our findings strongly suggest that exosomal LMP1 modulates endothelial functional properties responsible for tumor angiogenesis in an Akt/ERK pathway-dependent manner.

3.5 STIM1 knockdown inhibits angiogenesis in a chick embryo CAM xenograft model

We previously reported that STIM1-mediated signaling mediates EBV-facilitated tumor angiogenesis in NPC [18]. However, the remodeling of the original blood vessels induced by the transplanted NPC tumor has not been fully elucidated yet. The chick embryo CAM model established in our earlier work imitated realistic malignant profiles of tumor cells, such as growth, progression, and metastasis [26]. The CAM model also enables the visual and quantitative assessment of tumor angiogenesis in xenografts or transplanted primary NPC [26]. In this study, we developed this chick embryo CAM model with slight modifications to intuitively observe how the exosome-releasing NPC cells recruit ECs to form tumor-associated vasculature (Fig. 5a).

Five days after inoculation, the xenograft exhibited a visibly pro-angiogenic effect on vascular network formation, as compared with the Matrigel-control group. Radially grown vessels around the xenograft were generated in the CAMs (Fig. 5b), which were inhibited by STIM1 knockdown in HK1-EBV cells. In addition, the ratio of the vascularization area (VA) to the total CAM area was significantly reduced in the shRNA-STIM1 group (Fig. 5c). By performing section analysis with H & E staining, we observed intra-tumor neovascularization, which was defined as the newly-generated small-caliber vessels adjacent to the tumor cell clusters, and could even infiltrate the gaps between tumor cell clusters. The presence of embryonic nucleated erythrocytes in the lumen of the blood vessels allowed the tumor-associated vasculature to be recognized easily even without IHC (Fig. 5d). Intra-tumor neovascularization could be observed in 50% (5/10) of the shRNA-Ctrl. xenografts, but was seen in none of (0%, 0/10) the shRNA-STIM1 xenografts. The tumor-associated vasculature was further confirmed by IHC analysis of CD31, a classic endothelial marker (**Supplementary Fig. S1**). These results indicated that EBV-positive NPC cells reformed the original blood vessels by inducing secondary vasculature infiltration of the transplanted tumors in the CAMs. Inhibition of exosomal LMP1 delivery by silencing STIM1 in EBV-infected NPC cells partially eliminated the pro-angiogenic effect.

4 Discussion

Rapidly growing tumor cells need abundant blood carrying nutrients and oxygen, which allows dysregulated neoplastic proliferation, and accelerated tumor expansion requires an increasingly larger blood supply. Tumor angiogenesis sets up a vicious cycle of demand and supply. The recently emerged single-cell sequencing technology has revealed the landscape of tumor heterogeneity and the immune microenvironment in NPC, which is profoundly affected by latent EBV infection[7, 29, 30]. However, how EBV infection and its products modulate EC characteristics in the TME and facilitate angiogenesis and hematogenous dissemination remains understudied.

As a crucial intracellular second messenger, Ca^{2+} signaling regulates various cellular activities. Aberrantly activated SOCE is involved in tumor progression, angiogenesis, and metastasis and is clinically

associated with treatment resistance and clinical outcomes in human cancers [31]. Our earlier work showed that STIM1-dependent SOCE mediates tumor angiogenesis promotion by EBV infection in NPC [17, 18], but the pathway through which EBV-infected NPC cells manipulate endothelial phenotypes, remains unclear. In this study, we demonstrated that STIM1 regulates tumor angiogenesis by controlling the delivery of exosomal LMP1 to ECs in NPC. As a vital EBV-encoded functional oncoprotein, LMP1 has been implicated in the regulation of tumor angiogenesis through various approaches. For instance, LMP1 stimulates multiple regulators of pro-angiogenic factors and induces the production of molecules, such as IL-8, FGF-2, and VEGF [32–35]. LMP1 promotes the formation of vasculogenic mimicry in NPC through VEGFA/VEGFR1 signaling [36]. In addition, LMP1 can be transferred to ECs through exosomes secreted by EBV-infected cells, including NPC cells [12].

Endogenous LMP1 in EBV-infected host cells can escape degradation by accumulating in the luminal vesicles of multivesicular endosomes and further released into the external space via exocellular secretion in exosomes (Fig. 6) [37]. CD63 is a tetraspanin protein enriched in late endosomes, lysosomal compartments, and exosomal membranes [37]. LMP1 enrichment in exosomes and its secretion have been associated with CD63, whose knockdown results in reduced LMP1 enrichment in exosomes [38]. In our study, exosomal CD63 derived from NPC cells transfected with shRNA-STIM1 was comparable to that from shRNA-Ctrl. cells, suggesting that STIM1 regulates LMP1 enrichment in exosomes via a CD63-independent pathway. The endosomal-lysosomal sorting pathway plays a key role in exosome biogenesis and cargo sorting. This pathway involves ubiquitination, lipid sorting, and recognition by endosomal sorting complexes required for transport [39]. However, sorting LMP1 into exosomes does not require the lipid raft anchoring domain FWLY or N-terminal ubiquitination [37]. On one hand, LMP1 mediates proper intracellular trafficking through its C-terminus, whose modifications impair intracellular LMP1 trafficking and export via exosomes [37]. On the other hand, deletion of the N-terminus and transmembrane segments 1–2 or 1–4 of LMP1 impair its trafficking into exosomes, and the LMP1 C-terminus is not necessary for its enrichment [40]. The main limitation of our study is that the molecular structure domains through which STIM1 signaling regulates LMP1 enrichment into exosomes have not yet been fully addressed, mostly because of the complexity of the LMP1 sorting mechanism. This challenging issue needs to be solved in future studies.

In the present study, STIM1 knockdown inhibited the delivery of exosomal LMP1 while restraining Akt/ERK pathway activation in HUVECs. Similarly, STIM1-mediated signaling in tumor cells also remotely manipulates the Akt/ERK pathway in ECs [41]. STIM1 silencing promotes the enrichment of exosomal miR-145 released from breast cancer cells and inhibits insulin receptor substrate 1 and Akt/ERK signaling in ECs [41]. In addition to the Akt/ERK pathway, Akt can activate other downstream signaling molecules to promote angiogenesis. Akt activates endothelial nitric oxide synthase, a key regulator of EC proliferation, migration, and survival, which in turn stimulates nitric oxide production and induces angiogenesis [42, 43].

As the tumor progresses, angiogenesis provides the nutrients and oxygen needed for its uncontrolled growth *in situ*, offers an indispensable path for locoregional invasion, and supports distant metastatic

colonization. Our findings indicate that the exosomes harboring EBV-encoded LMP1 released by NPC cells enhance EC proliferation, migration, tubulogenesis, and permeability through an Akt/ERK-dependent pathway (Fig. 6). STIM1 regulates tumor angiogenesis by manipulating exosomal LMP1 enrichment. In addition, we further developed our CAM xenograft model for characterizing tumor angiogenesis in NPC, which enables a three-dimensional analysis of intra-tumor neovascularization. Utilizing this model, we showed that STIM1 knockdown reverses exosomal LMP1-promoted angiogenesis *in vivo*. This indicates that blockage of the exosomal delivery of EBV-associated pro-oncogenic biomolecules could serve as a feasible strategy for targeted therapy in NPC.

Abbreviations

STIM1, stromal interaction molecule 1; NPC, nasopharyngeal carcinoma; EBV, Epstein-Barr virus; LMP1, latent membrane protein 1; HNSCC, head and neck squamous cell carcinoma; TME, tumor microenvironment; ECs, endothelial cells; SOCE, store-operated Ca^{2+} entry; CAM, chorioallantoic membrane; FBS, fetal bovine serum; NTA, nanoparticle tracking analysis; HUVECs, human umbilical vein endothelial cells; PBS, phosphate-buffered saline; CCK-8, Cell Counting Kit-8; EdU, 5-ethynyl-2'-deoxyuridine; FITC, fluorescein isothiocyanate.

Declarations

Acknowledgments

We sincerely thank Prof. Sai-Wah Tsao (Hong Kong University) and Prof. Musheng Zeng (Sun Yat-sen University Cancer Center) for the gift of NPC cell lines.

Authors' contributions

J. Wei and J. Zhang conceived and designed the study. Y. Deng, J. Wei, and J. Zhang wrote the manuscript and prepared the figures. Y. Deng, X. Liu, Y. Huang, J. Ye, Y. Luo, Y. Chen, and Q. Li performed the experiments. Y. Deng, Q. He, Y. Lin, R. Liang, Y. Li, J. Wei, and J. Zhang analyzed the results. All the authors reviewed drafts of the paper and approved the submission of the manuscript.

Funding

This work was supported by the National Natural Science Foundation of China [grant numbers 82002859, 82073004, 81602390]; the Guangxi Natural Science Foundation [grant numbers 2020GXNSFBA297024, 2020GXNSFBA297059]. The sponsors have no role in the study design, data collection/analysis, manuscript writing, or the decision to submit the paper for publication.

Data availability statement

The original data supporting the conclusion of our article will be available from the corresponding authors upon reasonable request.

Ethical approval and consent to participate

This study was approved by the ethics committee of Guangxi Medical University Cancer Hospital (Ref: KY2020014), and informed consent was obtained from all patients. This study complied with the principles of the Declaration of Helsinki. All animal experiments performed in this study were approved by the Animal Research Committee of Guangxi Medical University and carried out according to the regulations of the Animal Research Committee of Guangxi Medical University.

Consent for publication

Not applicable.

Competing interests

The authors declare no conflict of interest.

References

1. Y.P. Chen, A.T.C. Chan, Q.T. Le, P. Blanchard, Y. Sun, J. Ma, Nasopharyngeal carcinoma. Lancet. 394, 64-80 (2019)
2. K.C.W. Wong, E.P. Hui, K.W. Lo, W.K.J. Lam, D. Johnson, L. Li, Q. Tao, K. C.A. Chan, K.F. To, A.D. King, B.B.Y. Ma, A.T.C. Chan, Nasopharyngeal carcinoma: an evolving paradigm. Nat Rev Clin Oncol. 18, 679-695 (2021)
3. R. Zheng, S. Zhang, H. Zeng S. Wang, K. Sun, R. Chen, L. Li, W. Wei, J. He, Cancer incidence and mortality in China, 2016. J Natl Cancer Cent. 2, 1-9 (2022)
4. W. Chen, R. Zheng, P. D. Baade, S. Zhang, H. Zeng, F. Bray, A. Jemal, X. Q. Yu, J. He, Cancer statistics in China, 2015. CA Cancer J Clin. 66, 115-132 (2016)
5. T. Yoshizaki, S. Kondo, K. Endo, Y. Nakanishi, M. Aga, E. Kobayashi, N. Hirai, H. Sugimoto, M. Hatano, T. Ueno, K. Ishikawa, N. Wakisaka, Modulation of the tumor microenvironment by Epstein-Barr virus latent membrane protein 1 in nasopharyngeal carcinoma. Cancer Sci. 109, 272-278 (2018)
6. L. Zhang, K.D. MacIsaac, T. Zhou, P.Y. Huang, C. Xin, J.R. Dobson, K. Yu, D.Y. Chiang, Y. Fan, M. Pelletier, Y. Wang, S. Jaeger, V. Krishnamurthy Radhakrishnan, L. JeBailey, P. Skewes-Cox, J. Zhang, W. Fang, Y. Huang, H. Zhao, Y. Zhao, E. Li, B. Peng, A. Huang, G. Dranoff, P.S. Hammerman, J. Engelman, H. Bitter, Y.X. Zeng, Y. Yao, Genomic Analysis of Nasopharyngeal Carcinoma Reveals TME-Based Subtypes. Mol Cancer Res. 15, 1722-1732 (2017)
7. S. Jin, R. Li, M.Y. Chen, C. Yu, L.Q. Tang, Y.M. Liu, J.P. Li, Y.N. Liu, Y.L. Luo, Y. Zhao, Y. Zhang, T.L. Xia, S.X. Liu, Q. Liu, G.N. Wang, R. You, J.Y. Peng, J. Li, F. Han, J. Wang, Q.Y. Chen, L. Zhang, H.Q. Mai, B.E.

Gewurz, B. Zhao, L.S. Young, Q. Zhong, F. Bai, M.S. Zeng, Single-cell transcriptomic analysis defines the interplay between tumor cells, viral infection, and the microenvironment in nasopharyngeal carcinoma. Cell Res. 30, 950-965 (2020)

8. S.C. Liu, N.M. Tsang, P.J. Lee, Y.H. Sui, C.H. Huang, T.T. Liu, Epstein-Barr Virus Induces Adipocyte Dedifferentiation to Modulate the Tumor Microenvironment. Cancer Res. 81, 3283-3294 (2021)
9. X. Liu, Y. Deng, Y. Huang, J. Ye, S. Xie, Q. He, Y. Chen, Y. Lin, R. Liang, J. Wei, Y. Li, J. Zhang, Nasopharyngeal Carcinoma Progression: Accumulating Genomic Insta vcxzzbility and Persistent Epstein-Barr Virus Infection. Curr Oncol. 29, 6035-6052 (2022)
10. N.A. Giraldo, R. Sanchez-Salas, J.D. Peske, Y. Vano, E. Becht, F. Petitprez, P. Validire, A. Ingels, X. Cathelineau, W.H. Fridman, C. Sautès-Fridman, The clinical role of the TME in solid cancer. Br J Cancer. 120, 45-53 (2019)
11. Y. Huang, M. Kanada, J. Ye, Y. Deng, Q. He, Z. Lei, Y. Chen, Y. Li, P. Qin, J. Zhang, J. Wei, Exosome-mediated remodeling of the tumor microenvironment: From local to distant intercellular communication. Cancer Lett. 543, 215796 (2022)
12. D.G. Jr, Meckes, K.H. Shair, A.R. Marquitz, C.P. Kung, R.H. Edwards, N. Raab-Traub, Human tumor virus utilizes exosomes for intercellular communication. Proc Natl Acad Sci U S A. 107, 20370-20375 (2010)
13. A.A. Benders, W. Tang, J.M. Middeldorp, A.E. Greijer, L.B. Thorne, W.K. Funkhouser, W. K. Rathmell, M.L. Gulley, Epstein-Barr virus latent membrane protein 1 is not associated with vessel density nor with hypoxia inducible factor 1 alpha expression in nasopharyngeal carcinoma tissue. Head Neck Pathol. 3, 276-282 (2009)
14. A. Kieser, K.R. Sterz, The Latent Membrane Protein 1 (LMP1). Curr Top Microbiol Immunol. 391, 119-149 (2015)
15. C. Keryer-Bibens, C. Pioche-Durieu, C. Villemant, S. Souquère, N. Nishi, M. Hirashima, J. Middeldorp, P. Busson, Exosomes released by EBV-infected nasopharyngeal carcinoma cells convey the viral latent membrane protein 1 and the immunomodulatory protein galectin 9. BMC Cancer. 6, 283 (2006)
16. J. Wei, J. Zhang, Y. Si, M. Kanada, Z. Zhang, S. Terakawa, H. Watanabe, Blockage of LMP1-modulated store-operated Ca^{2+} entry reduces metastatic potential in nasopharyngeal carcinoma cell. Cancer Lett. 360, 234-244 (2015)
17. J. Ye, J. Huang, Q. He, W. Zhao, X. Zhou, Z. Zhang, Y. Li, J. Wei, J. Zhang, Blockage of store-operated Ca^{2+} entry antagonizes Epstein-Barr virus-promoted angiogenesis by inhibiting Ca^{2+} signaling-regulated VEGF production in nasopharyngeal carcinoma. Cancer Manag Res. 10, 1115-1124 (2018)
18. J. Ye, J. Wei, Y. Luo, Y. Deng, T. Que, X. Zhang, F. Liu, J. Zhang, X. Luo, Epstein-Barr Virus Promotes Tumor Angiogenesis by Activating STIM1-Dependent Ca^{2+} Signaling in Nasopharyngeal Carcinoma. Pathogens. 10, 1275 (2021)
19. S.W. Messenger, S.S. Woo, Z. Sun, T.F.J. Martin, A Ca^{2+}-stimulated exosome release pathway in cancer cells is regulated by Munc13-4. J Cell Biol. 217, 2877-2890 (2018)

20. A. Savina, C.M. Fader, M.T. Damiani, M.I. Colombo, Rab11 promotes docking and fusion of multivesicular bodies in a calcium-dependent manner. Traffic. 6, 131-143 (2005)
21. A. Savina, M. Furlán, M. Vidal, M.I. Colombo, Exosome release is regulated by a calcium-dependent mechanism in K562 cells. J Biol Chem. 278, 20083-20090 (2003)
22. Y. Chen, R. Koshy, E. Guirado, A. George, STIM1 a calcium sensor promotes the assembly of an ECM that contains Extracellular vesicles and factors that modulate mineralization. Acta Biomater. 120, 224-239 (2021)
23. S.Y. Chan, K.W. Choy, S.W. Tsao, Q. Tao, T. Tang, G.T. Chung, K.W. Lo, Authentication of nasopharyngeal carcinoma tumor lines. Int J Cancer. 122, 2169-2171 (2008)
24. M.J. Strong, M. Baddoo, A. Nanbo, M. Xu, A. Puetter, Z. Lin, Comprehensive high-throughput RNA sequencing analysis reveals contamination of multiple nasopharyngeal carcinoma cell lines with HeLa cell genomes. J Virol. 88, 10696-10704 (2014)
25. J. Wei, J. Ye, Y. Luo, J. Weng, Q. He, F. Liu, M. Li, Y. Lin, Y. Li, Z. Zhang, S. Qu, J. Zhang, EB virus promotes metastatic potential by boosting STIM1-dependent Ca^{2+} signaling in nasopharyngeal carcinoma cells. Cancer Lett. 478, 122-132 (2020)
26. X. Xiao, X. Zhou, H. Ming, J. Zhang, G. Huang, Z. Zhang, P. Li, Chick Chorioallantoic Membrane Assay: A 3D Animal Model for Study of Human Nasopharyngeal Carcinoma. PLoS One. 10, e0130935 (2015)
27. J. Wang, Q. Jiang, O.D. Faleti, C.M. Tsang, M. Zhao, G. Wu, S.W. Tsao, M. Fu, Y. Chen, T. Ding, T. Chong, Y. Long, X. Yang, Y. Zhang, Y. Cai, H. Li, M. Peng, X. Lyu, X. Li, Exosomal Delivery of AntagomiRs Targeting Viral and Cellular MicroRNAs Synergistically Inhibits Cancer Angiogenesis. Mol Ther Nucleic Acids. 22, 153-165 (2020)
28. A.K. Lo, C.W. Dawson, H.L. Lung, K.L. Wong, L.S. Young, The Role of EBV-Encoded LMP1 in the NPC Tumor Microenvironment: From Function to Therapy. Front Oncol. 11, 640207 (2021)
29. J. Zhao, C. Guo, F. Xiong, J. Yu, J. Ge, H. Wang, Q. Liao, Y. Zhou, Q. Gong, B. Xiang, M. Zhou, X. Li, G. Li, W. Xiong, J. Fang, Z. Zeng, Single cell RNA-seq reveals the landscape of tumor and infiltrating immune cells in nasopharyngeal carcinoma. Cancer Lett. 477, 131-143 (2020)
30. Y. Liu, S. He, X.L. Wang, W. Peng, Q.Y. Chen, D.M. Chi, J.R. Chen, B.W. Han, G.W. Lin, Y.Q. Li, Q.Y. Wang, R.J. Peng, P.P. Wei, X. Guo, B. Li, X. Xia, H.Q. Mai, X.D. Hu, Z. Zhang, Y.X. Zeng, J.X. Bei, Tumour heterogeneity and intercellular networks of nasopharyngeal carcinoma at single cell resolution. Nat Commun. 12, 741 (2021)
31. J. Wei, Y. Deng, J. Ye, Y. Luo, J. Weng, Q. He, F. Liu, M. Li, R. Liang, Y. Lin, Y. Li, J. Zhang, J. Yang, S. Qu, Store-operated Ca^{2+} entry as a key oncogenic Ca^{2+} signaling driving tumor invasion-metastasis cascade and its translational potential. Cancer Lett. 516, 64-72 (2021)
32. Z. Wang, F. Luo, L. Li, L. Yang, D. Hu, X. Ma, Z. Lu, L. Sun, Y. Cao, STAT3 activation induced by Epstein-Barr virus latent membrane protein1 causes vascular endothelial growth factor expression and cellular invasiveness via JAK3 And ERK signaling. Eur J Cancer. 46, 2996-3006 (2010)

33. N. Wakisaka, S. Murono, T. Yoshizaki, M. Furukawa, J.S. Pagano, Epstein-barr virus latent membrane protein 1 induces and causes release of fibroblast growth factor-2. Cancer Res. 62, 6337-6344 (2002)
34. T. Yoshizaki, T. Horikawa, R. Qing-Chun, N. Wakisaka, H. Takeshita, T.S. Sheen, S.Y. Lee, H. Sato, M. Furukawa, Induction of interleukin-8 by Epstein-Barr virus latent membrane protein-1 and its correlation to angiogenesis in nasopharyngeal carcinoma. Clin Cancer Res. 7, 1946-1951 (2001)
35. S. Murono, H. Inoue, T. Tanabe, I. Joab, T. Yoshizaki, M. Furukawa, J.S. Pagano, Induction of cyclooxygenase-2 by Epstein-Barr virus latent membrane protein 1 is involved in vascular endothelial growth factor production in nasopharyngeal carcinoma cells. Proc Natl Acad Sci U S A. 98, 6905-6910 (2001)
36. S. Xu, J. Bai, Z. Zhuan, B. Li, Z. Zhang, X. Wu, X. Luo, L. Yang, EBV-LMP1 is involved in vasculogenic mimicry formation via VEGFA/VEGFR1 signaling in nasopharyngeal carcinoma. Oncol Rep. 40, 377-384 (2018)
37. F.J. Verweij, M.A. van Eijndhoven, E.S. Hopmans, T. Vendrig, T. Wurdinger, E. Cahir-McFarland, E. Kieff, D. Geerts, R. van der Kant, J. Neefjes, J.M. Middeldorp, D.M. Pegtel, LMP1 association with CD63 in endosomes and secretion via exosomes limits constitutive NF-κB activation. EMBO J. 30, 2115-2129 (2011)
38. S.N. Hurwitz, D. Nkosi, M.M. Conlon, S.B. York, X. Liu, D.C. Tremblay, D.G. Jr, Meckes, CD63 Regulates Epstein-Barr Virus LMP1 Exosomal Packaging, Enhancement of Vesicle Production, and Noncanonical NF-κB Signaling. J Virol. 91, e02251-16 (2017)
39. R.C. Piper, J.P. Luzio, Ubiquitin-dependent sorting of integral membrane proteins for degradation in lysosomes. Curr Opin Cell Biol. 19, 459-465 (2007)
40. D. Nkosi, L.A. Howell, M.R. Cheerathodi, S.N. Hurwitz, D.C. Tremblay, X. Liu, D.G. Jr, Meckes, Transmembrane Domains Mediate Intra- and Extracellular Trafficking of Epstein-Barr Virus Latent Membrane Protein 1. J Virol. 92, e00280-18 (2018)
41. S. Pan, X. Zhao, C. Shao, B. Fu, Y. Huang, N. Zhang, X. Dou, Z. Zhang, Y. Qiu, R. Wang, M. Jin, D. Kong, STIM1 promotes angiogenesis by reducing exosomal miR-145 in breast cancer MDA-MB-231 cells. Cell Death Dis. 12, 38 (2021)
42. S. Goetze, A. Bungenstock, C. Czupalla, F. Eilers, P. Stawowy, U. Kintscher, C. Spencer-Hänsch, K. Graf, B. Nürnberg, R. E. Law, E. Fleck, M. Gräfe, Leptin induces endothelial cell migration through Akt, which is inhibited by PPAR gamma-ligands. Hypertension. 40, 748-754 (2002)
43. A. Uruno, A. Sugawara, H. Kanatsuka, S. Arima, Y. Taniyama, M. Kudo, K. Takeuchi, S. Ito, Hepatocyte growth factor stimulates nitric oxide production through endothelial nitric oxide synthase activation by the phosphoinositide 3-kinase/Akt pathway and possibly by mitogen-activated protein kinase kinase in vascular endothelial cells. Hypertens Res. 27, 887-895 (2004)

Figures

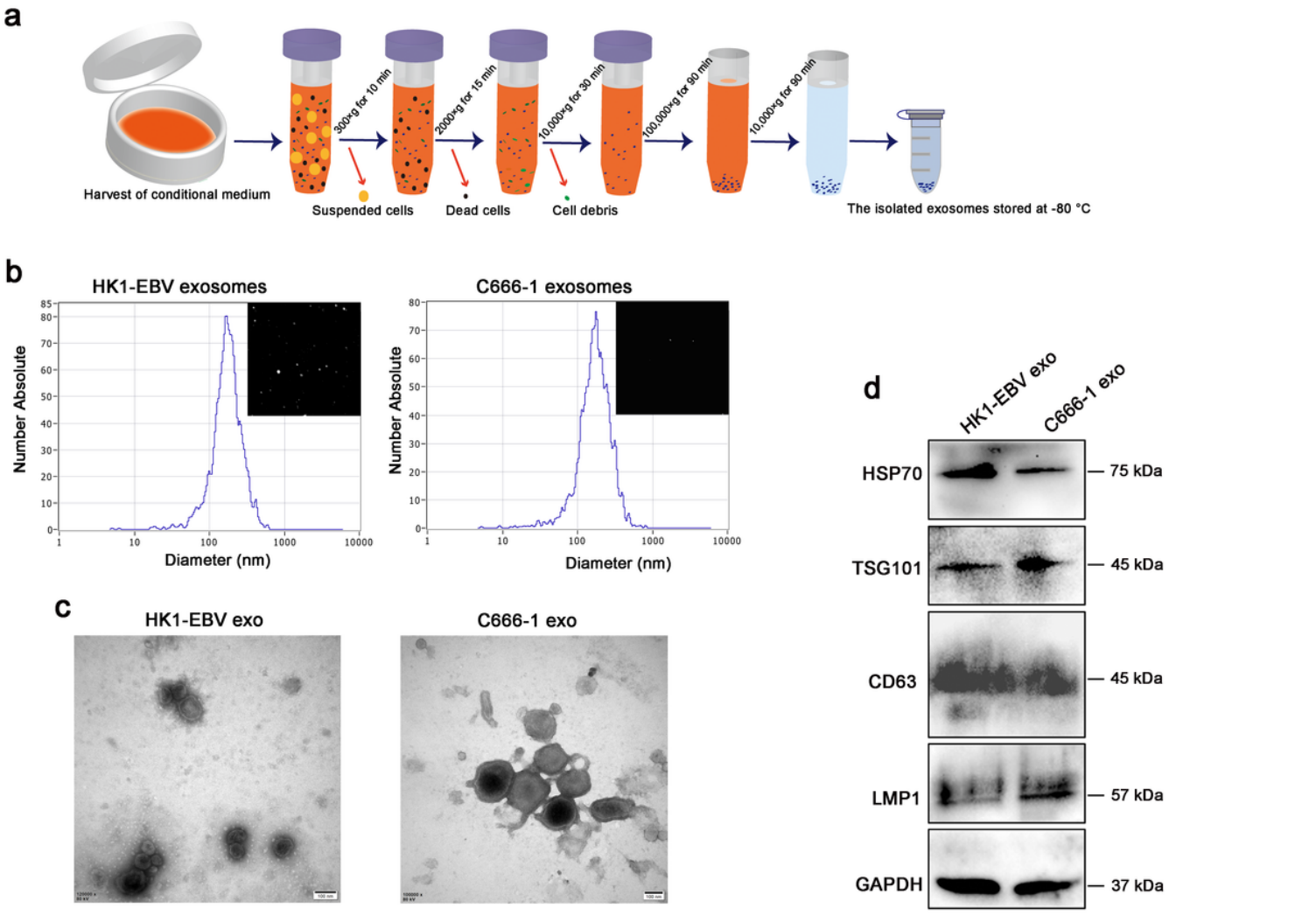

Figure 1

The exosomes released by Epstein-Barr virus (EBV)-positive nasopharyngeal carcinoma (NPC) cells carry latent membrane protein 1 (LMP1) (**a**) Scheme of exosome isolation and enrichment via differential ultracentrifugations. (**b**) Particle size distribution of the NPC cell-derived exosomes was determined via nanoparticle tracking analysis. (**c**) Representative transmission electron microscopy photographs of the exosomes released by HK1-EBV or C666-1 cells. Bar = 100 nm. (**d**) Western blotting of exosomal markers and EBV-LMP1. GAPDH served as an in-house control. All the experiments were conducted in triplicates.

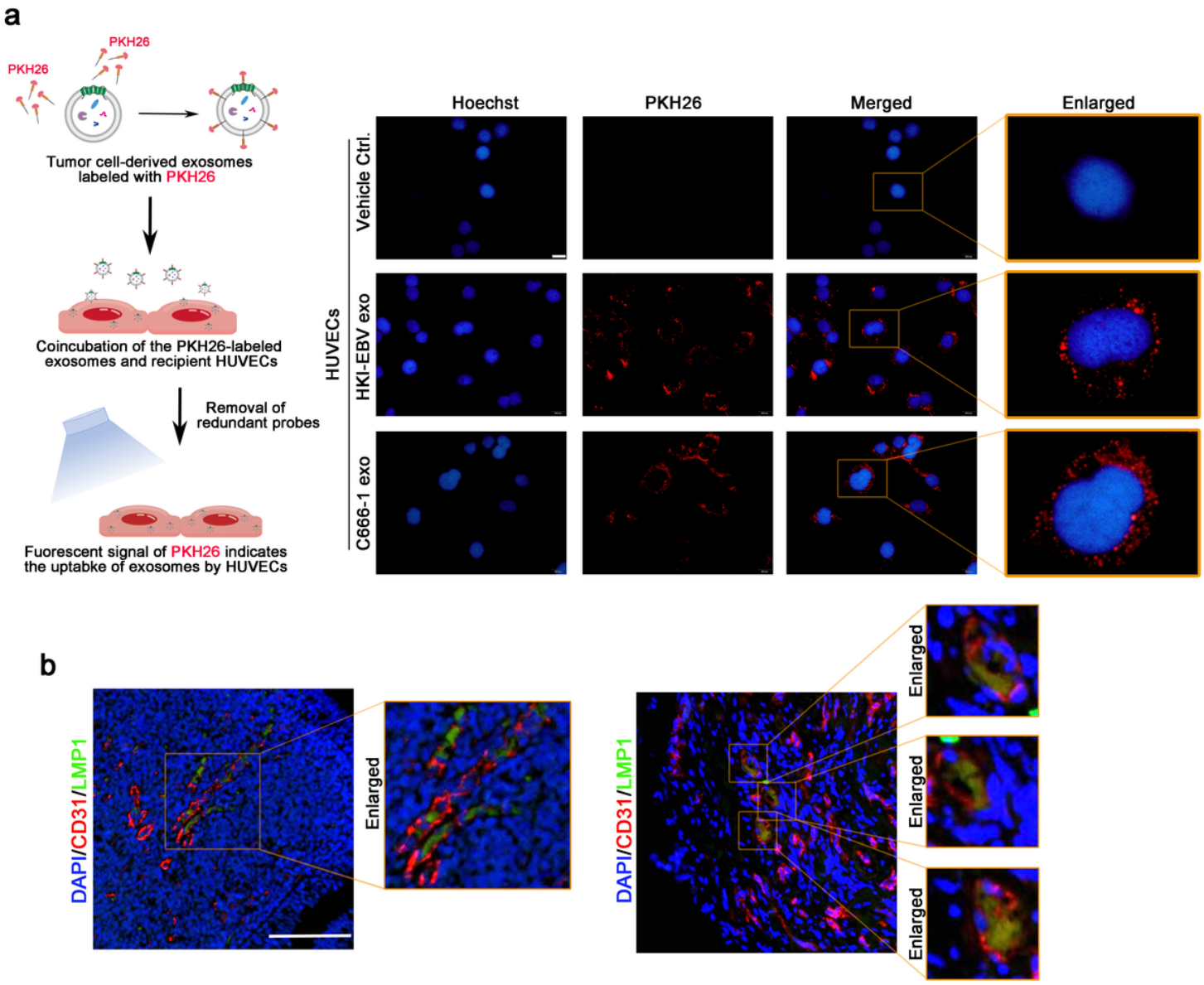

Figure 2

Endothelial cells (ECs) can uptake exosomes harboring LMP1 and clinically correlate with tumor angiogenesis in NPC. (**a**) Schematic diagram illustrating the protocol for detecting fluorescent probe-labeled exosomes uptaken by ECs (left panel). PKH26 was employed as a fluorescent indicator of the tumor cell-derived exosome uptake by human umbilical vein endothelial cells (HUVECs) (right panel). Bar = 20 μm. The experiments were conducted in triplicates. (**b**) Two representative immunofluorescent photographs showing CD31 and LMP1 colocalization in NPC tissues. Bar = 100 μm.

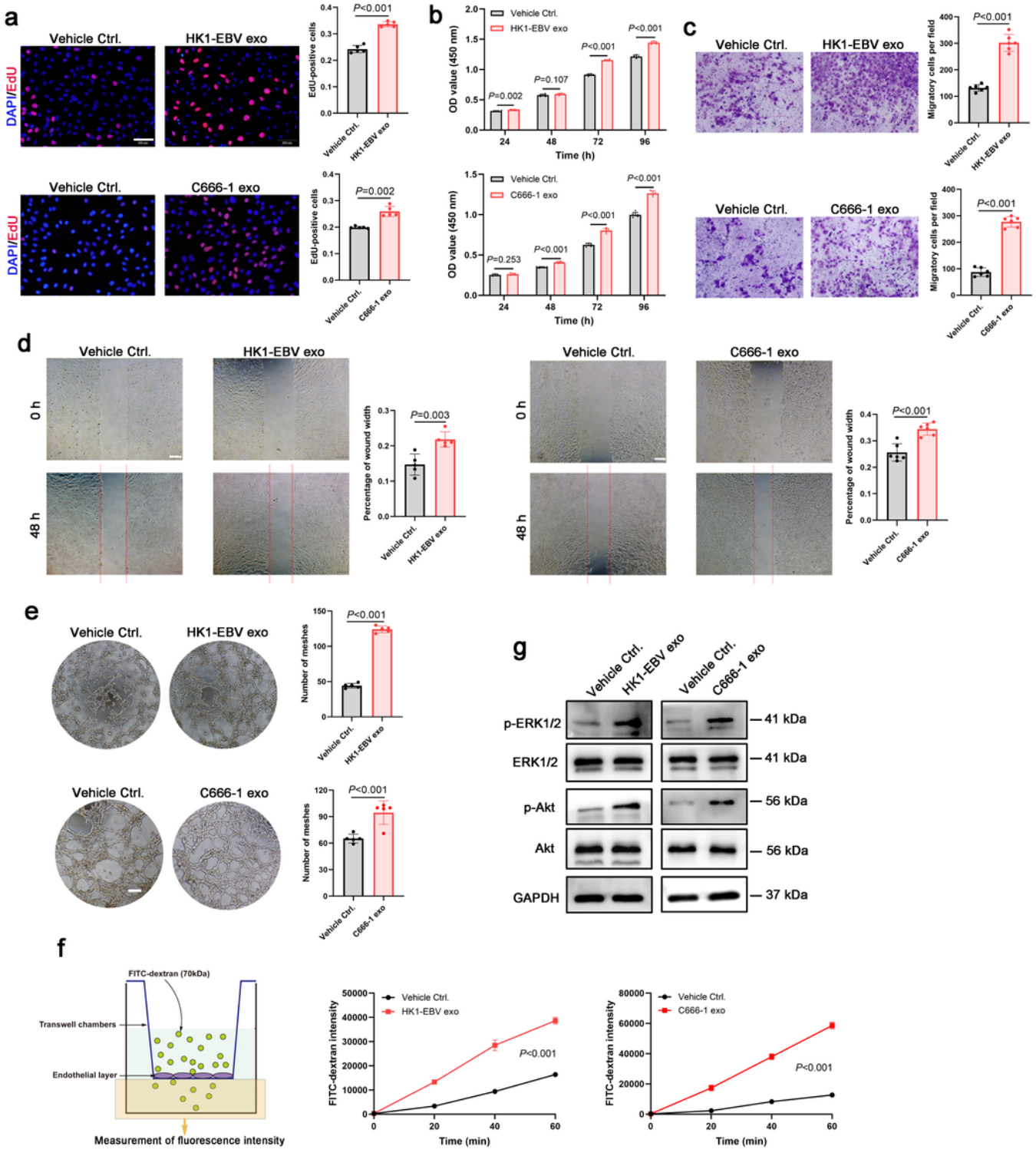

Figure 3

Exosomes carrying LMP1 promote proliferation, migration, tubulogenesis, and permeability through the Akt/ERK pathway in ECs. (**a**) Proliferation of HUVECs incubated with or without the NPC cell-derived exosomes was measured via 5-ethynyl-2'-deoxyuridine (EdU) fluorescence staining. Phosphate-buffered saline (PBS) served as vehicle control (vehicle-Ctrl.). Bar = 200 μm. Histograms indicate the number of EdU-positive cells per random field (Student's *t*-test). (**b**) HUVEC viability in the presence or absence of

NPC cell-derived exosomes was evaluated via the Cell Counting Kit-8 (CCK-8) assay in the indicated time points (Student's *t*-test). (**c**) HUVEC transwell migration assay. Histograms in the right panels indicate the quantification of migratory cells across the membrane (Student's *t*-test). (**d**) A wound healing assay was performed to elucidate the migration of HUVECs incubated with or without exosomes. Histograms indicate the quantitative analysis of cell migration in each right panel (Student's *t*-test). Bar = 200 μm. (**e**) Tube formation assay was carried out to evaluate HUVEC angiogenic capacity in the absence or presence of exosomes. Representative photographs of HUVEC tube formation are shown. Histograms show the quantitative analysis of endothelial tubulogenesis (Student's *t*-test). Bar = 200 μm. (**f**) The permeability of the HUVEC-formed layer treated with or without exosomes was determined via the fluorescein isothiocyanate-dextran (FITC-Dextran) permeability assay (two-way ANOVA). (**g**) Western blotting of AKT, p-AKT, ERK1/2, and p-ERK1/2 in HUVECs pre-incubated with or without exosomes. GAPDH was used as an in-house control. Data are presented as means ± SD. All the experiments were conducted in triplicates.

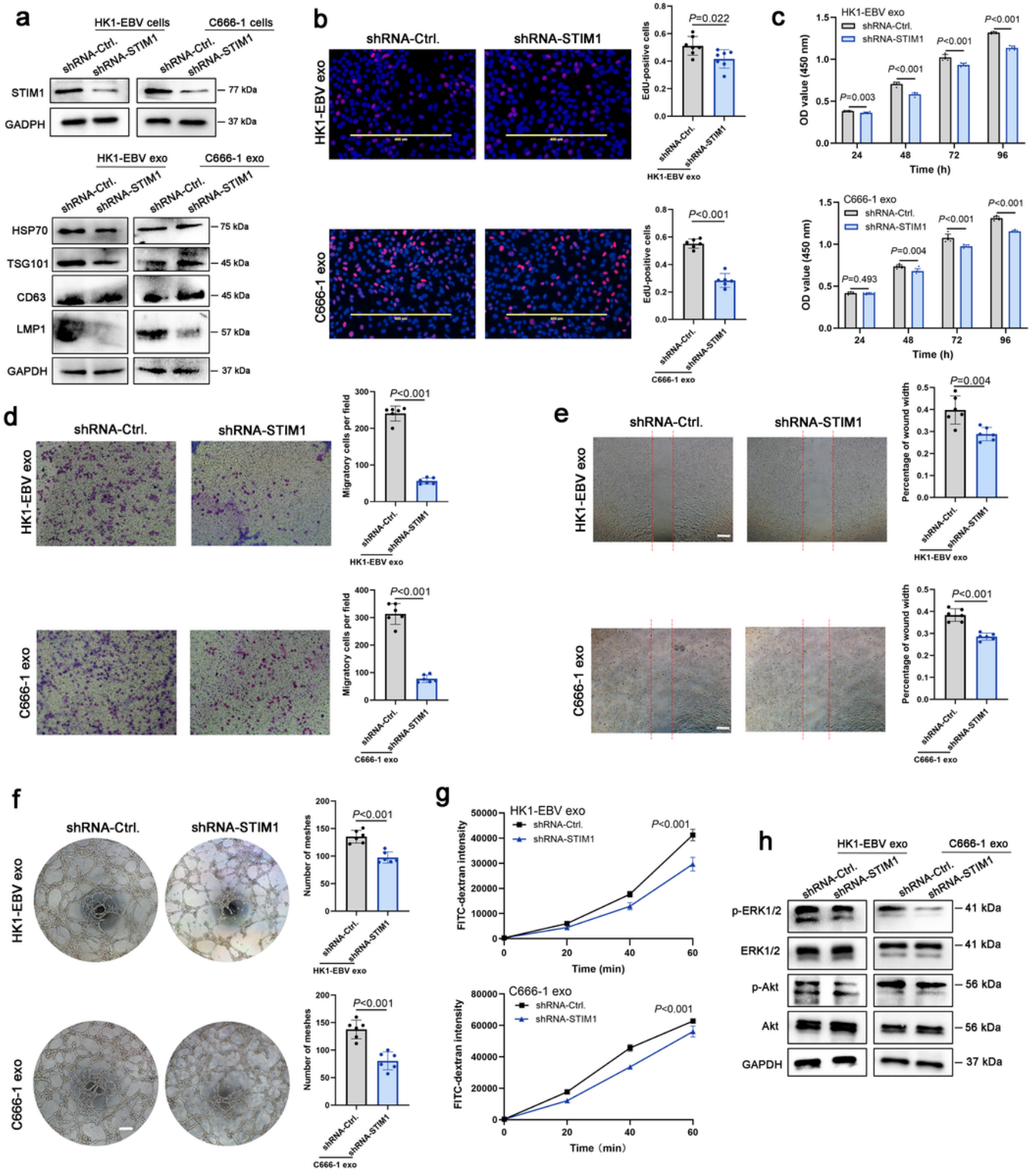

Figure 4

Stromal interaction molecule 1 (STIM1) silencingblunts the effects of NPC cell-derived exosomes on endothelial features by reducing LMP1 delivery. (**a**) The effective knockdown of STIM1 in NPC cells was confirmed via western blotting (upper panel). The amounts of various exosomal makers and LMP1 enrichment were evaluated in the exosomes derived from the vector-control (shRNA-Ctrl.) or STIM1-knockdown(shRNA-STIM1)(bottom panel). (**b**) Proliferation of HUVECs incubated with exosomes derived

from the shRNA-control or shRNA-STIM1 cells was determined via EdU fluorescence staining (Student's *t*-test).Bar = 400 μm. (**c**) The viability of HUVECs incubated with the indicated exosomes was measured via the CCK-8 assay (Student's *t*-test). (**d**) Transwell assay for migration of HUVECs treated with the exosomes as indicated. (**e**) Wound healing assay for migration of HUVECs incubated with the exosomes released by the shRNA-Ctrl. or shRNA-STIM1 NPC cells (Student's *t*-test). Bar = 200 μm. (**f**) Tube formation assay for the angiogenic capacity of HUVECs (Student's *t*-test). Bar = 200 μm. (**g**) FITC-Dextran assay for the permeability of HUVECs treated with exosomes from the indicated NPC cells (two-way ANOVA). **(h**) The expression levels of AKT, p-AKT, ERK1/2, and p-ERK1/2 in the HUVECs pre-incubated with exosomes derived from shRNA-Ctrl. or shRNA-STIM1 NPC cells. Data are presented as means ± SD. All the experiments were conducted in triplicates.

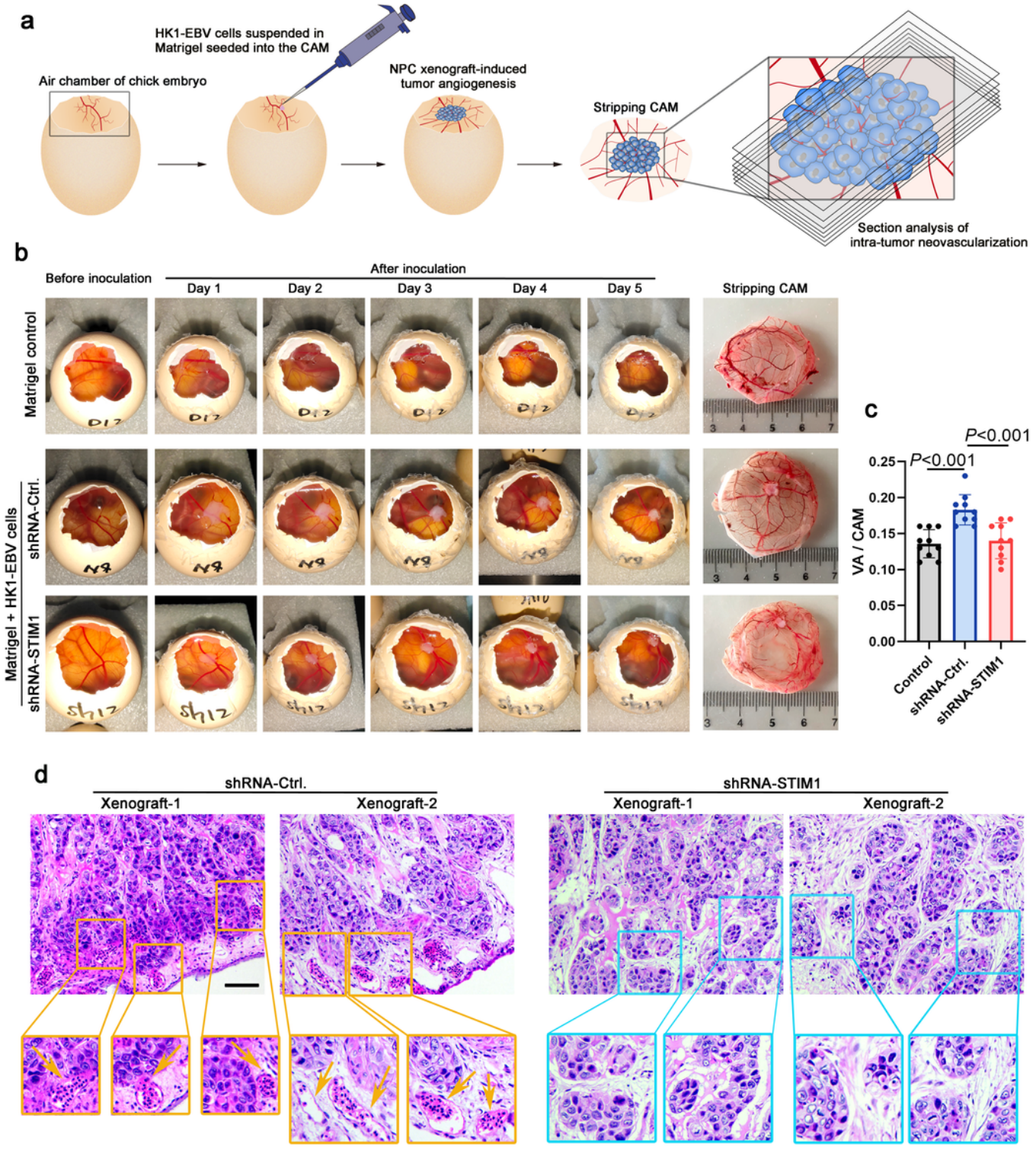

Figure 5

STIM1 knockdown inhibits tumor angiogenesis in the chick embryo chorioallantoic membrane (CAM) xenograft model. (**a**) Schematic diagram illustrating the establishment of the CAM xenograft model for analyzing tumor angiogenesis and intra-tumor neovascularization. CAMs were inoculated with the suspended shRNA-Ctrl. or shRNA-STIM1 HK1-EBV cells with Matrigel. Five days post-inoculation, the CAMs were separated and subjected to routine fixation, followed by hematoxylin and eosin (H & E)

staining. (**b**) Representative photographs of shRNA-Ctrl. or shRNA-STIM1 xenograft in the CAMs. The transplanted tumor-induced vascular network formation is shown in the striping CAMs. (**c**) Tumor angiogenesis quantification by calculating the ratio of the vascularized area (VA) against the total CAM area. Data are presented as means ± SD (Student's *t*-test). (**d**) Representative images of the shRNA-Ctrl. or shRNA-STIM1 xenografts with H & E staining. Yellow arrows denote the newly-generated small-caliber tumor-associated vasculature adjacent to the tumor cell clusters. The embryonic nucleated erythrocytes are present in the intravascular lumen. Bar = 200 μm.

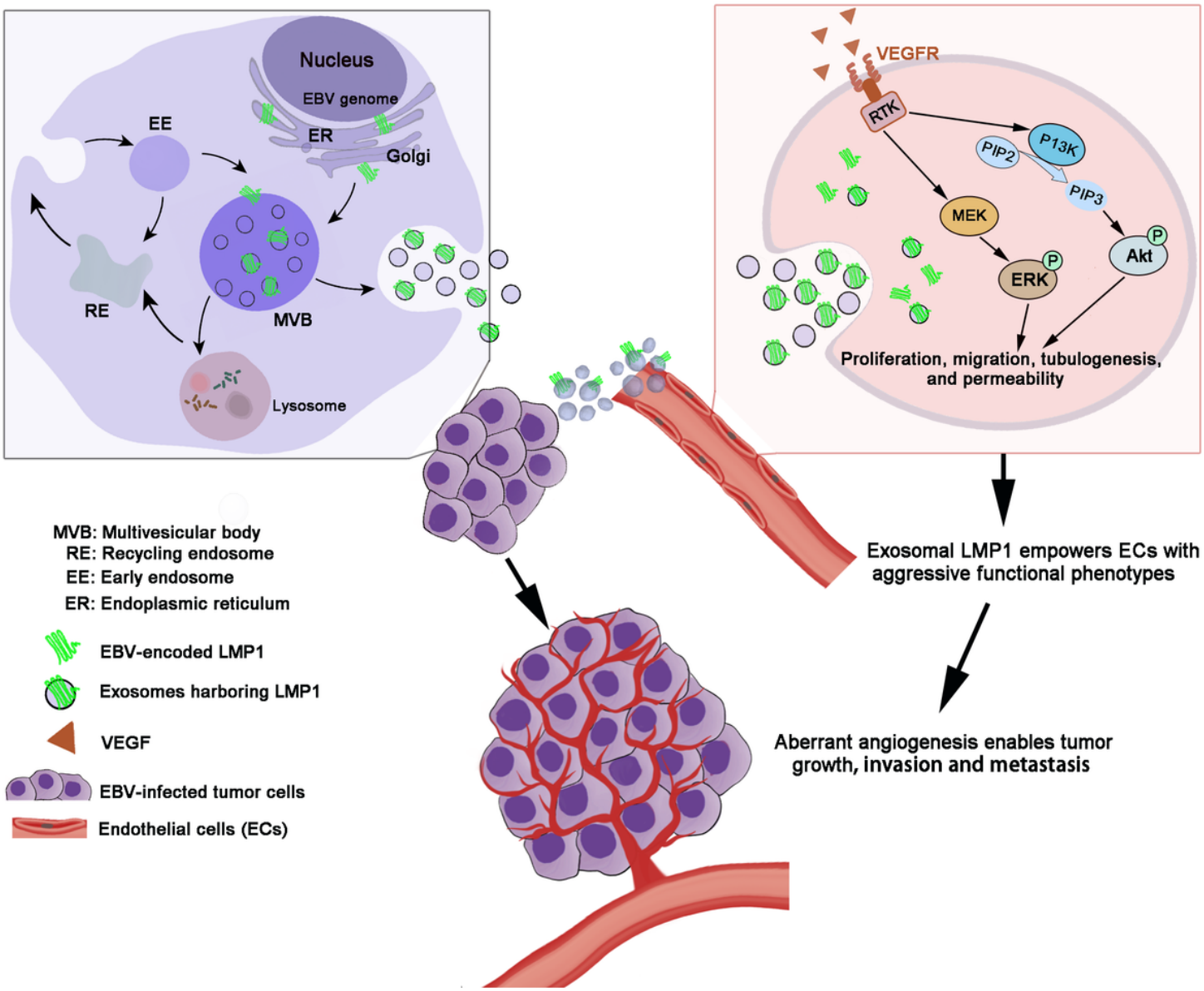

Figure 6

Schematic diagram illustrating the intercellular communication between NPC cells and ECs in the tumor microenvironment (TME). In this proposed model, EBV-infected NPC cells mobilize surrounding ECs via the delivery of LMP1-enriched exosomes, which is regulated by STIM1. Exosomal LMP1 endows ECs with aggressive functional characteristics through the Akt/ERK pathway. The "aggressive" ECs thus contribute to the remodeling of original vascular and intra-tumor neovascularization.

Supplementary Files

This is a list of supplementary files associated with this preprint. Click to download.

- SupplementaryFigureLegend.docx
- SupplementaryFigureS1.tif
- SupplementaryFigureS2.zip
- SupplementaryFigureS3.zip
- SupplementaryFigureS4.zip
- SupplementaryFigureS5.zip